Eddy Current and Temperature Field Computation in Transverse Flux Induction Heating Equipment for Galvanizing Line

Zanming Wang, Xiaoguang Yang, Youhua Wang, and Weili Yan

***Abstract*—This paper describes the 3-D eddy current FEM computation of transverse flux inductors used for heating strip in galvanized steel productions. The adopted mathematical model consists of a differential equation system for the steady-state eddy current problem and a Fourier's thermal conduction equation for moved media. The finite element method is applied in conjunction with the Galerkin method. The simplifications and boundary conditions required for an efficient solution are discussed.**

***Index Terms*—3-D FEM, eddy current field, temperature field, transverse flux induction heating.**

I. Introduction

INDUCTION heating processes for heating galvanized steel trips provide significant technological, economic and ecological advantages in comparison with conventional oil-or gas-fired furnace: fast heating rate, instant controllability, high efficient and minimal environment pollution. To achieve a completely uniform temperature across the entire strip width is consequently a critical factor in the development of a practical TFIH. The design of the TFIH equipment necessitates accurate process performance prediction for the thermal characteristic.

A 3-D FEM eddy current and temperature field simulation is used for developing such equipment. It is essential to obtain a clear understanding of the induced current (eddy current) in the workpiece and further more the power losses in temperature field. With the developing of computer and numerical computation techniques it is now possible. Fig. 1 shows the construction of steel galvanizing line and Fig. 2 is our experiment model of the TFIH equipment.

II. Mathematical Model

The problem considered here is that of eddy currents at low angular frequencies ω. The displacement current is ignored. Magnetic permeability μ and electric conductivity κ are assumed to be constant over longer periods of time (several cycles of the field-exciting voltages). The influence of the movement of strip to the magnetic field distribution is very small and can be neglected.

The mathematical model for this sinusoidal steady-state eddy current problem results from the Maxwell equations and

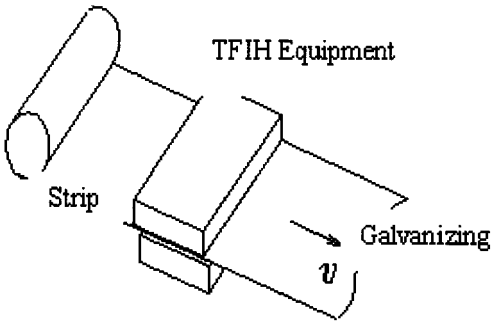

Fig. 1. Concise construction figure of steel galvanizing making line.

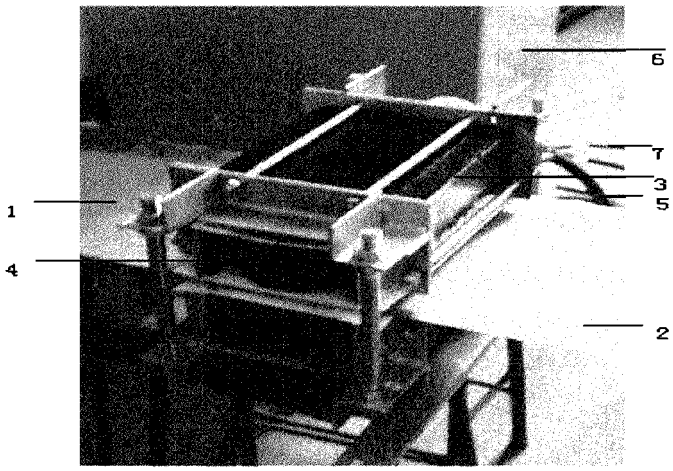

Fig. 2. Experiment model of the TFIH equipment, where 1 is the strip before heating, 2 the strip after heating, 3 yoke, 4 coil, 5 power wire, 6 middle frequency power, and 7 cooling water pipe.

is described by means of the complex magnetic vector potential $\underline{\vec{A}}$ and a complex scalar potential $\underline{\phi}$:

$$\operatorname{rot}\frac{1}{\mu}\operatorname{rot}\underline{\vec{A}}+j\omega\kappa\left(\underline{\vec{A}}-\operatorname{grad}\underline{\phi}\right)=\kappa\underline{\vec{E}}_s. \tag{1}$$

$\vec{E}_S$ is the electric field strength impressed by the power source. Moreover, the requirement of a source-free eddy current density must be fulfilled

$$\operatorname{div}\kappa\left(\underline{\vec{A}}-\operatorname{grad}\underline{\phi}\right)=0. \tag{2}$$

The magnetic vector potential $\underline{\vec{A}}$ builds up in the vicinity of electric conductors. For designing an adequate distance from

Manuscript received June 5, 2000.

This work was supported by the Chinese Education Ministry and the Science and Technology Department of Hebei Provincial Government.

X. Yang is with the Hebei University of Technology, 300130 Tianjin, China (e-mail: yangxg@eyou.com).

Publisher Item Identifier S 0018-9464(01)07838-4.

the inductor, it can, however, be assumed that this potential is negligibly small and the boundary condition

$$\underline{\vec{A}} = 0 \tag{3}$$

is applicable. In contrast to the vector potential, the gradient of the potential ϕ must only computed in the conductive areas. On the surfaces of these conductive area the boundary condition

$$\left(\underline{\vec{A}} - \operatorname{grad} \underline{\phi}\right) \cdot \vec{n} = 0 \tag{4}$$

must be fulfilled. The 3-D solution area thus determined is further determined if necessary in case there are symmetries or asymmetries of the electromagnetic field.

The current density is

$$\underline{\vec{J}} = j\omega\kappa \left(\underline{\vec{A}} - \operatorname{grad} \underline{\phi}\right) + \kappa \underline{\vec{E}}_s \tag{5}$$

which determines the heat source distribution

$$p_v = \left|\underline{\vec{J}}^2\right| \Big/ \kappa. \tag{6}$$

The temperature field $\vartheta(x, y, z)$ is computed on the basis of the Fourier's thermal conduction equation

$$\frac{\partial(c\rho\vartheta)}{\partial t} = \operatorname{div}(\lambda \operatorname{grad} \vartheta) + p_v - \vec{v} \operatorname{grad}(c\rho\vartheta) \tag{7}$$

where

- λ is the thermal conductivity coefficient,
- c the specific heat,
- ρ the mass density, and
- $\vec{v}$ the strip velocity respectively.

This temperature field must only be computed for the workpiece. Thermal losses by convection and radiation on the strip surface are considered with the Cauchy boundary condition

$$\lambda \operatorname{grad} \vartheta \cdot \vec{n} = \alpha(\vartheta_o - \vartheta) \tag{8}$$

where α is the heat transfer-coefficient for convection and radiation and ϑ_o the ambient temperature respectively.

Furthermore, at an adequate distance from the inductor, boundary conditions must be determined over the cross section of the workpiece.

On the side on which the strip enters the solution area, temperatures (e.g., ambient temperature) are given. On the exit side, however

$$\operatorname{grad} \vartheta \cdot \vec{n} = 0 \tag{9}$$

is indicated where $\vec{n}$ corresponds to the velocity direction. The two fields, the electromagnetic field and the temperature field which becomes steady-state at constant velocity, are coupled via the temperature dependence of the electric conductivity $\kappa(x, y, z)$ and the magnetic permeability $\mu(x, y, z)$. This coupling is, however, relatively weak, because it is relatively easy to do with iterative functions for $\mu(x, y, z)$ and $\kappa(x, y, z)$.

III. Boundary Condition

The computation of the electromagnetic field by approximation is performed on the basis of the finite element method. The Galerkin method is applied to (1) and (2), duly considering the boundary and symmetry conditions [1]–[4].

For initial computations for orientation purposes, the reaction of the temperature field and the influence of the supply feeds (connecting leads) on the electromagnetic field are preferably neglected. Under these assumptions, three planes of symmetry can be defined. This reduces the solution area to 1/8 of the total volume.

In the x–z and the y–z planes of symmetry, the electric current densities are oriented perpendicular to them, respectively. Hence on the x–z plane the components of the magnetic vector potential $\underline{\vec{A}}$ and the scalar potential $\underline{\phi}$ are

$$\underline{\vec{A}}_X = \underline{\vec{A}}_Z = 0 \tag{10}$$

$$\frac{\partial \underline{\vec{A}}_Y}{\partial y} = 0 \tag{11}$$

$$\underline{\phi} = 0 \tag{12}$$

and on the y–z plane

$$\underline{\vec{A}}_y = \underline{\vec{A}}_Z = 0 \tag{13}$$

$$\frac{\partial \underline{\vec{A}}_x}{\partial x} = 0 \tag{14}$$

$$\underline{\phi} = 0. \tag{15}$$

On the x–y plane of symmetry, the current density has no perpendicular component and

$$\underline{\vec{A}}_z = 0 \tag{16}$$

$$\frac{\partial \underline{\vec{A}}_x}{\partial x} = \frac{\partial \underline{\vec{A}}_y}{\partial y} = 0 \tag{17}$$

$$d\underline{\phi}/dn = 0. \tag{18}$$

IV. Eddy Current and Heat Sources

The eddy current density can be worked out with the magnetic potential $\underline{\vec{A}}$ and the electrical scalar potential as equation (19)

$$\underline{\vec{J}} = k\left(j\omega \underline{\vec{A}} - \nabla \underline{\varphi}\right) \tag{19}$$

written in component form:

$$\underline{\vec{J}}_x = k\left(j\omega \underline{\vec{A}}_x - \nabla \underline{\varphi}_x\right) \tag{20}$$

$$\underline{\vec{J}}_y = k\left(j\omega \underline{\vec{A}}_y - \nabla \underline{\varphi}_y\right) \tag{21}$$

$$\underline{\vec{J}}_z = k\left(j\omega \underline{\vec{A}}_z - \nabla \underline{\varphi}_z\right). \tag{22}$$

The ohmic power loss, which is expressed by the eddy current density in the workpiece, can be computed with the

$$p_v = \tfrac{1}{2} \underline{\vec{J}} \cdot \underline{\vec{J}}^* / k. \tag{23}$$

V. Results

Fig. 3 shows the mesh of the 1/8 of the overall computation domain. The width varies from 0.35∼0.40 m, from 8 to 60 m/min.

The calculated eddy current distribution on the strip surface is illustrated in Fig. 4. Because the depth of current penetration

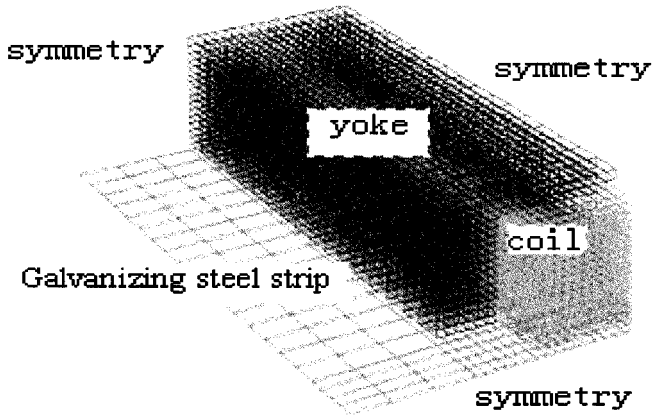

Fig. 3. Mesh element in 1/8 area.

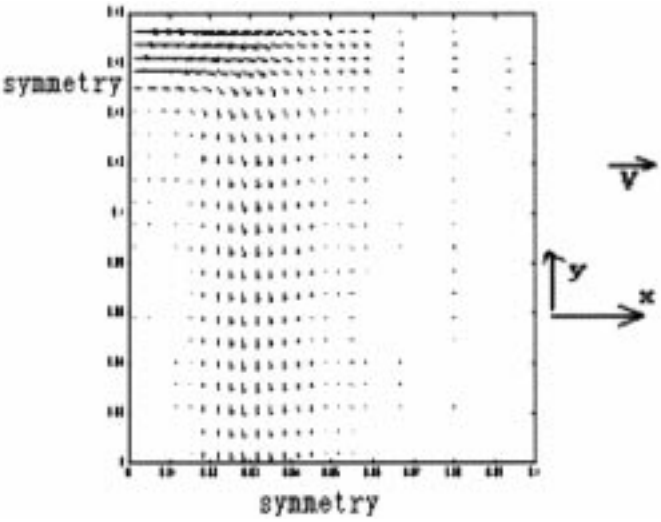

Fig. 4. Eddy current distribution on the 1/4 strip surface, where the arrow length represents eddy current intensity.

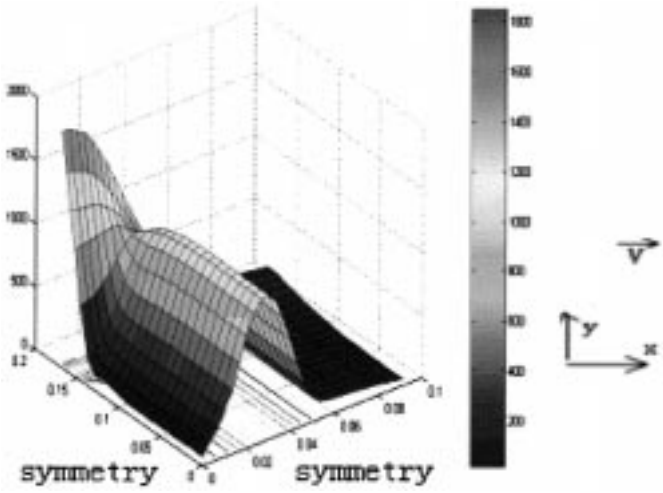

Fig. 5. Distribution of heat source density (w/cm^3) in 1/4 area.

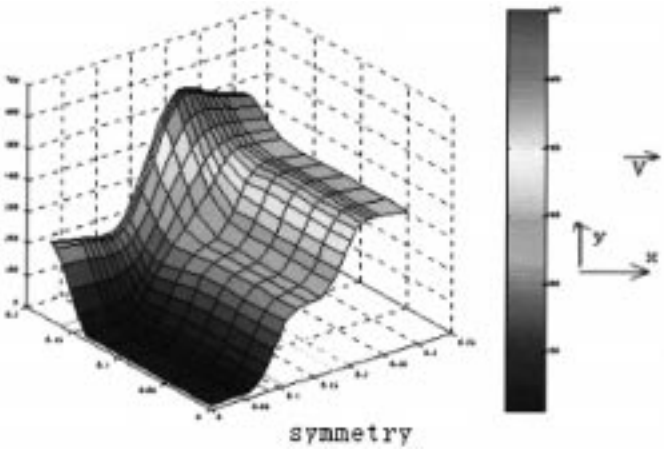

Fig. 6. Steady-state temperature distribution (in □).

is much greater than the strip width, a similar eddy current distribution will also occur in the deeper layers.

The computation of the temperature field of the moving strip is done on the basis of a particular grid. The heat source distribution, in the form of node values, is transferred to this grid by means of the shape functions. The influence of the velocity destroys the coefficient matrix symmetry of the equation system. A biconjugate gradient procedure was therefore adopted as solution method. The density of heat source distribution according to equation (23) is shown in Fig. 5.

Fig. 6 shows the temperature distribution resulting from the reflected heat sources distribution as per Fig. 5 in the steady-state situation. The computed results are confirmed by temperature measurements performed with an infrared camera.

VI. Conclusions

In the design of TFIH equipment the computation of eddy current and heat source distributions are beneficial for theoptimum choosing of the design parameters in order to obtain a high efficient and homogenous heating across the strip, the exactly control of the working process varies from different workpieces by means of the numerical predication model under the industry conditions.

References

[1] Z. Wang *et al.*, "3D multifields FEM computation of transverse flux induction heating for moving-strips," *IEEE Trans. Magn.*, vol. 35, no. 3, pp. 1642–1645, May 1999.

[2] Z. Wang, "Modellierung und optimaler Entwurf der Querfelderwaermung," Ph.D. dissertation, Technical University of Ilmenau, Germany, 1996.

[3] D. Schulze, Z. Wang, and B. Nachke, "Development an universal TFIH equipment using 3d eddy current field computation," *IEEE Trans. Magn.*, vol. 32, no. 3, pp. 1609–1612, May 1996.

[4] W. Andree, D. Schulz, and Z. Wang, "3D FEM eddy current computation in transverse flux induction heating equipment," *IEEE Trans. Magn.*, vol. 30, no. 4, July 1994.